Experiments on VIV Under Frequency Modulation and at Constant Reynolds Numbers

Conference Paper · January 2008

DOI: 10.1115/OMAE2008-57957

4 authors:

Guilherme Rosa Franzini
University of São Paulo
74 PUBLICATIONS **336** CITATIONS
SEE PROFILE

Adriano Axel
Warsaw School of Economics
4 PUBLICATIONS **9** CITATIONS
SEE PROFILE

André L. C. Fujarra
Federal University of Santa Catarina, Joinville, Brazil
122 PUBLICATIONS **835** CITATIONS
SEE PROFILE

Celso P. Pesce
University of São Paulo
147 PUBLICATIONS **871** CITATIONS
SEE PROFILE

Proceedings of OMAE'08:
27th International Conference on Offshore Mechanics and Arctic Engineering
15-20 June 2008, Estoril, Portugal

OMAE2008-57957

EXPERIMENTS ON VIV UNDER FREQUENCY MODULATION AND AT CONSTANT REYNOLDS NUMBERS

Guilherme R. Franzini[2]
(guilherme.franzini@gmail.com)

Adriano A. P. Pereira[2]
(adriano.axel@gmail.com)

André L.C. Fujarra[2]
(afujarra@usp.br)

Celso P. Pesce[1]
(ceppesce@usp.br)

LIFE&MO - Fluid-Structure Interaction and Offshore Mechanics Laboratory

[1]Department of Mechanical Engineering
[2]Department of Naval Architecture and Ocean Engineering

Escola Politécnica
University of São Paulo
São Paulo, SP, Brazil

ABSTRACT

The present paper presents a new mechanical apparatus, specially designed for investigating fundamental aspects of VIV in a Towing Tank. An electrically driven movable spring-leaf system was conceived and constructed to deal with elastic mounted cantilevered cylinders, either rigid or flexible ones. The apparatus has low structural damping and allows the excitation of VIV under continuously modulated spring rigidity, aiming at investigating the effect of natural frequency modulation on the response. The experiments were carried out at IPT Towing Tank, which is 280m long, 6m wide and 4m deep. Both rigid and flexible cantilevered cylinders mounted on the new apparatus were studied. In this paper, some results on the rigid cylinder are presented. A striking feature of such apparatus is the possibility to obtain the whole VIV amplitude and frequency response curves from a single run, under a single towing velocity, therefore at the same Reynolds number. This is possible as the reduced velocity varies along that particular constant velocity run, according to the natural frequency modulation.

Keywords: VIV, frequency modulation, experimental device, Hilbert-Huang spectral analysis, Reynolds number

INTRODUCTION

Vortex Induced Vibration (VIV) is a key matter in the design of marine structures, particularly important in the fatigue life evaluation of risers and tendons. A massive effort has been done in this last two decades, aiming at addressing the subject from both points of view: fundamentals and practical applications.

Nonetheless, many points remain open. The co-existence of multi-mode vibrations at a single frequency, as observed from laboratory experiments by Chaplin et al [1], and from full-scale tests, recently discussed as ´frequency time-sharing´ by Swithenbank et al [2], is just one of various intriguing aspects of VIV and its consequences. Examples of questions that still puzzle academia and industry are: Reynolds number dependence, Govardhan and Williamson [3]; standing and/or traveling waves and the importance of high harmonics response on fatigue life, Vandiver [4]; jumps and mode switching, triggered by tension oscillation due to first and second-order wave-motions of the floating unit, Silveira et al [5]; modal riser response identification; Lucor and Triantafyllou [6], Kassen [7].

The deeper VIV research goes into all those conceptual and practical points, more important fundamental studies turn

to be. Special experimental techniques, comprising both devices and analysis methods, should be devised as those introduced by Hover et al. [8], who used force feed-back systems combined with on-line numerical simulations to study VIV of mounted cylinders and cables.

This paper introduces a new experimental apparatus envisaged to investigating the effect of natural frequency modulation on the response, aiming at enlightening the effect of tension modulation in VIV of marine risers.

THE NEW EXPERIMENTAL APPARATUS

Figure 1 shows the new[1] experimental apparatus. It is a variable-span spring-leaf system that can deal with elastic mounted cantilevered cylinders, either rigid or flexible ones. The device allows crosswise vibrations only and was designed, considering IPT towing tank characteristics, to cover a particular range of reduced velocities and frequency modulations. FEA and genetic algorithm techniques guided the design towards an improved performance.

Figure 1. The new experimental apparatus. Left, picture. Right CAD plot.

A conventional electric system (step-motor driven) controls the vertical position of the clamp, through a central, long and very small pitch screw. This makes the spring-leaves rigidity to vary according the clamp position, enabling to modulate the first natural frequency of the system in crosswise direction.

The present apparatus can be instrumented in various ways. Strain-gages may be placed on the spring-leaves, enabling to identify their vibration; Fujarra and Pesce [10]. Accelerometers may be fixed to the lower rigid plate or inside the cylinder. The motion of the lower plate may be tracked optically. For the 'rigid' cylinder assembling, a single transversal accelerometer may be used to measure the crosswise oscillation.

[1] One of the reviewers brought to the authors attention the existence of a similar apparatus [9], designed for a different purpose: to study the propulsion mechanism of a variable-length spring fin. That device works immersed, though.

Specially constructed flexible cylinders, Pesce and Fujarra [11], or having a metallic internal bar, Fujarra et al [12], may be instrumented with inside accelerometers or even with strain-gages, to obtain stream and crosswise vibrations. Details on the design and instrumentation will be subject of a specific paper.

Geometric and dynamic parameters

Table 1 shows the main geometric parameters of the device, in this case assembled to a 'rigid' cylinder. A further paper will explore the flexible cylinder mounting. The aspect ratio of the 'rigid' cylinder is 35.4 (immersed part).

Table 1. Geometric parameters.

Rigid Cylinder	
Material	Al alloy
External diameter (mm)	25.4
Internal diameter (mm)	23.4
Total length (mm)	1000
Immersed length (mm)	900
Spring-leaves	
Material	Al alloy
Maximum length (mm)	800
Minimum length (mm)	200
Width (mm)	100
Thickness (mm)	0.8
Lower rigid plate	
Material	Al alloy
Width (mm)	100
Length (mm)	100
Thickness (mm)	4

Table 2 shows the inertial parameters of this particular 'rigid' cylinder assembling.

Table 2. Mass parameters

Lower rigid plate mass (kg)	0.417
Rigid cylinder mass (kg)	0.227
Total moving structural mass (kg)	0.644
Mass ratio, m*	1.41

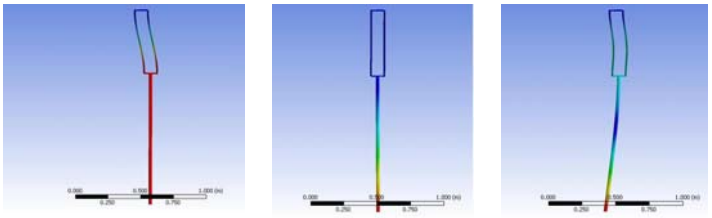

(1) (2) (3)

Figure 2. 'Rigid' cylinder mounted on the spring-leaves apparatus. The three first eigenmodes: 1.26, 10.01, 14.29Hz. Spring-leaves span: 485mm. FEM analysis.

Figure 2 shows the results of a numerical modal analysis in still water obtained with a common finite element method software. Added mass coefficient has been set to 1.12, which was determined after comparing results of experimental

decaying tests in air and water; see Pesce and Fujarra [11]. As can be seen, the first vibration mode is a 'rigid body' one, with a 1.26Hz eigenfrequency. The second eigenfrequency corresponds to the first pure bending mode of the 'rigid' cylinder (bending is minimal) and the third one shows simultaneous bending of the spring-leaves and the 'rigid' cylinder. The values of the second and third eigenfrequencies are high if compared to the first one and do not affect the dynamic phenomena at low towing speeds, at least not substantially.

Figure 3 shows the (crosswise) first natural frequency as a function of the span length L_s of the spring-leaves, measured from the clamp to the lower rigid plate where the cylinder is fixed. Table 3 shows the same values, compared to those from FEA.

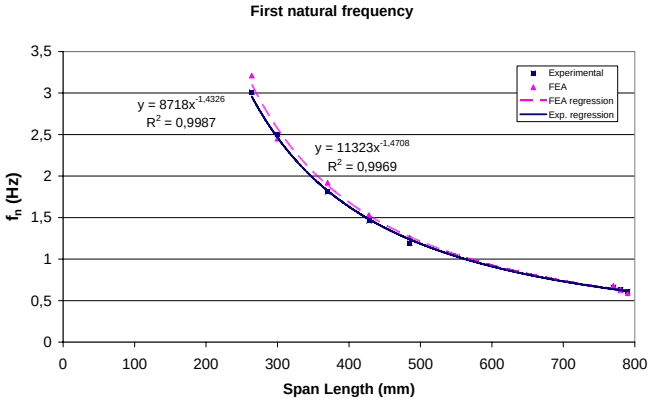

Figure 3. First Natural Frequency in Water as a function of spring-leaves span.

Table 3. Eigenfrequencies (Hz) in water. 'Rigid' cylinder mounted on spring-leaves apparatus.

Span (mm)	Experimental	FEA (*)
264	3.01	3.21
300	2.50	2.45
370	1.81	1.92
428	1.46	1.53
485	1.19	1.26
770	0.66	0.68
780	0.63	0.63
790	0.61	0.59

(*) added-mass coefficient: 1.12

The apparatus is low structural damped. In fact, the structural damping coefficient is very low, as shows the plot in Fig. 4, as a function of vibration amplitude, determined from several decaying tests with distinct span lengths. Typically, the structural damping coefficient is of order $\zeta \cong 0.1\%$ in air, at amplitude values of circa $A^* = A_y / D \cong 0.7$, leading to a mass-damping parameter lower than $\alpha = (m^* + C_a)\zeta \approx 0.025$, as defined in Govardhan and Williamson [3].

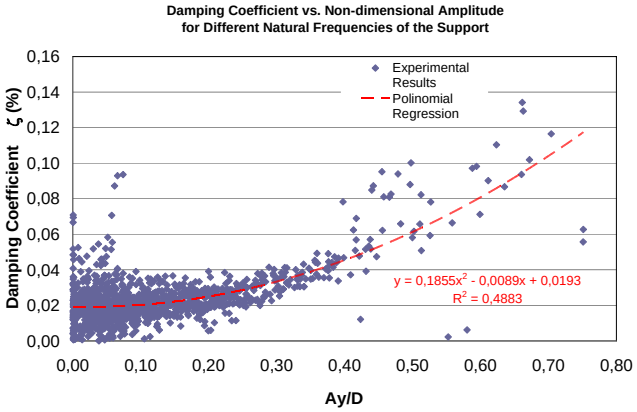

Figure 4. Structural damping coefficient from decaying tests at several natural frequencies.

THE HILBERT-HUANG SPECTRAL ANALYSIS TECHNIQUE

Usual VIV analysis techniques are statistical or linear spectral ones. However, their applicability may be questionable in some cases as VIV is a nonlinear fluid-elastic phenomenon and, not rare, oscillations signals are non-stationary. A discussion on this subject may be found in Pesce et al [13], where a novel technique, due to Huang et al [14], is applied to VIV phenomena. This technique will be once more explored, and shown to be particularly useful in obtaining the whole VIV response (amplitude and frequency curves) from a single run, under a single towing velocity, therefore at a constant Reynolds number. This is possible if the natural frequency is modulated in time, making the reduced velocity to vary during that particular constant velocity run. This technique will also be shown to be quite interesting for common VIV runs.

As pointed out in Pesce et al [13], and reproduced below, the Hilbert-Huang spectrum analysis was envisaged and developed by Huang et al. [14] as an alternative and powerful technique to deal with non-stationary signals that emerge from non-linear systems. This method applies the usual Hilbert transform to a finite set of 'Intrinsic Mode Functions[2]' (IMFs), obtained from the original signal through an 'Empirical Mode Decomposition' (EMD). According to those authors: "the name 'intrinsic mode function' is adopted because it represents the oscillation mode imbedded in the data". Let $X_j(t)$ be a specific IMF and $Z_j(t)$ an analytic function defined as

$$Z_j(t) = X_j(t) + iY_j(t) = a_j(t)\exp\left[i\theta_j(t)\right] \qquad (1)$$

where

$$Y_j(t) = \frac{1}{\pi} P \int_{-\infty}^{\infty} \frac{X_j(\tau)}{t-\tau} d\tau \qquad (2)$$

is the Hilbert Transform of $X_j(t)$; P stands for principal value.

[2] In the H-H technique, the intrinsic "mode" is a temporal one, not the structural "mode" (vibration eigenmode).

The original signal is then decomposed into the IMF set, as in a 'generalized Fourier series',

$$X(t) = \mathrm{Re}\sum_{j=1}^{n} a_j(t)\exp\left(i\int \omega_j(t)dt\right). \quad (3)$$

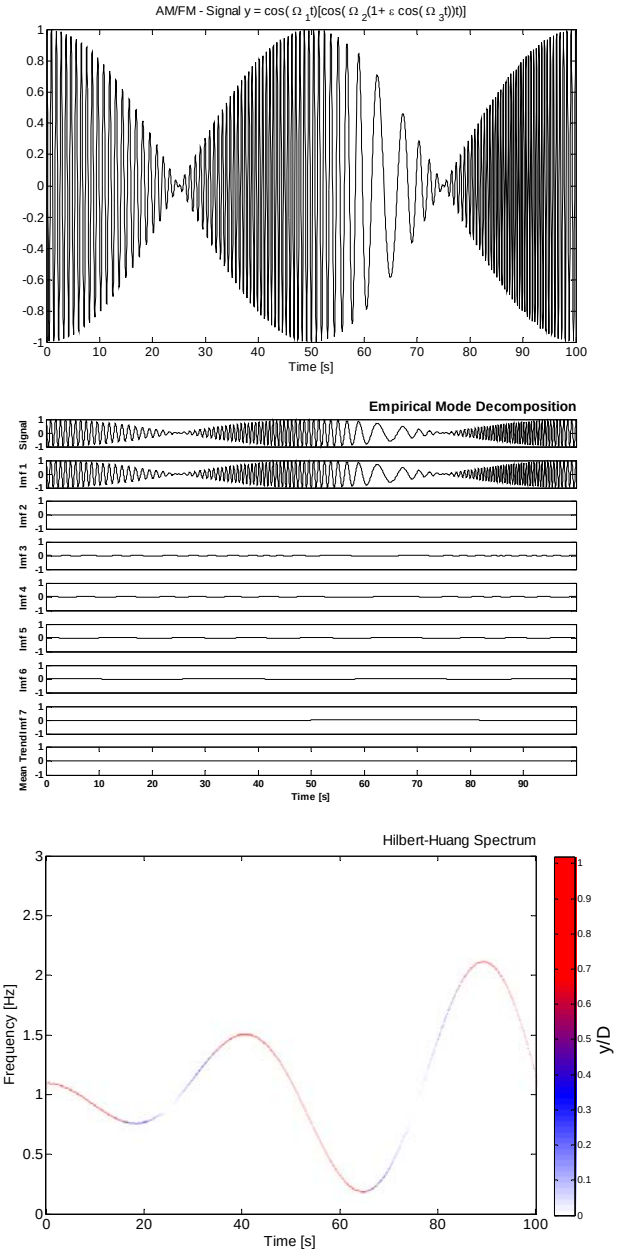

Figure 5. The Hilbert-Huang technique applied to a synthesized AM/FM signal (Eq. (5). Signal, Intrinsic mode functions (IMFs) and Spectrum.
$\Omega_1 = \Omega_2/100; \Omega_2 = 2\pi; \Omega_3 = \Omega_2/50; \varepsilon = 0.1$.

Not only the amplitude $a_j(t)$ but also the local phase $\theta_j(t)$, and so the local (or instantaneous) frequency,

$$\omega_j(t) = \frac{d}{dt}\left(\theta_j(t)\right), \quad (4)$$

characterizing each IMF, is time dependent. The concept of local frequency can be formalized through the stationary phase method, as pointed out in [14].

The EMD method, conceived to obtain the set of IMFs, is based on a recursive subtraction of successively means that are calculated between the two time-envelope of extrema (maxima and minima) contained in the signal. The envelopes are splines fitting of the maxima (and minima). Details can be found in [14], where this method is referred to as a 'sifting' process. Such a recursive procedure is carried out for each IMF limited by a standard deviation stopping criterion that is applied at each step. Each calculated IMF has, itself, symmetrical (maxima and minima) envelopes. The IMF set is complete, by construction. The orthogonality property was also shown numerically in [14]. The residual function coming out from this procedure is not an IMF; it is the (long-term) trend of the signal. The method precludes zero or mean references and is applicable to general transient signals. See, also, **Erro! Fonte de referência não encontrada.**.

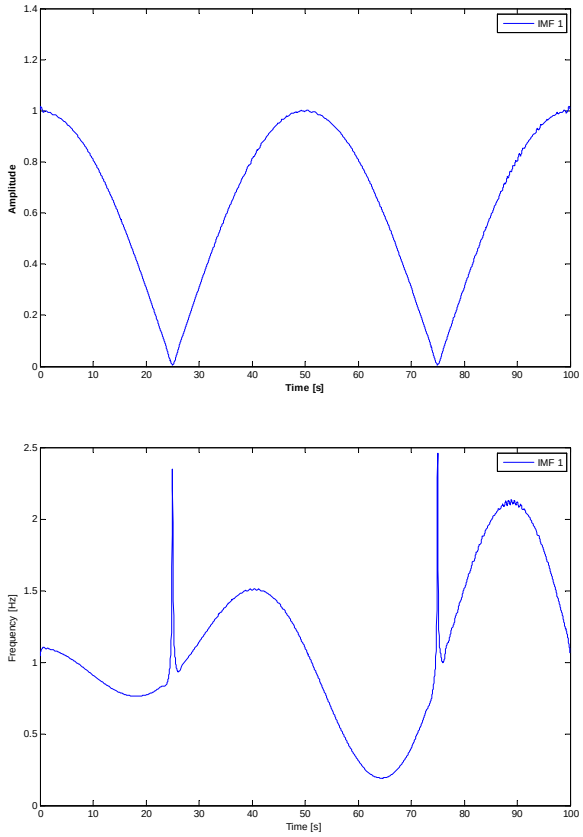

Figure 6. The Hilbert-Huang technique applied to a synthesized AM/FM signal. Amplitude and frequency traces.

In order to exemplify the use of such technique, Figures 5 and 6 show its application to a synthesized signal. This signal is amplitude and frequency modulated in the following form,

$$y(t) = \cos\Omega_1 t \cdot \left[\cos(\Omega_2 t(1+\varepsilon\cos\Omega_3 t)\right] \quad . \qquad (5)$$

For this synthesized signal, almost all energy is concentrated in the first IMF (intrinsic mode function). The modulated amplitude is a smooth curve, clearly shown in Fig. 6. The modulated frequency, also shown in Fig. 6, is a smooth curve, as well, except at the instants where the amplitude (so the energy of the signal) is very small (close to zero). Such (numerical) spikes are visually filtered out the spectrum (Fig. 5), where energy is presented according to a color scale.

EXPERIMENTAL RESULTS WITH A 'RIGID' CYLINDER

The amplitude was obtained by twice integrating in time an accelerometer signal, crosswise mounted on the rigid lower plate, combined to a first-order high-pass filtering technique, with a properly chosen cut-off frequency.

Runs at fixed spring-leaves span length

Firstly, the H-H technique is applied to usual VIV runs, having the spring-leaves span fixed, and varying the towing-tank carriage, therefore varying the reduced velocity. Amplitude and frequency VIV responses are presented in a standard plot, where the natural frequency is kept constant. In this case, reduced velocity is kept constant during each run, at a value,

$$V_r = \frac{U}{f_n D} \quad , \qquad (6)$$

where the natural frequency is the first eigenfrequency experimentally obtained form decaying tests in still water.

Figure 7 shows an example of VIV response, at a constant spring-leaf span length, $L_s = 485\text{mm}$. Well-known, the natural frequency varies according to the shedding pattern. Reduced velocity is here defined using the still water natural frequency $f_n = 1.19\text{Hz}$, with no correction regarding such a variation.

The response frequency response is completely recovered with the H-H technique, by simply taken the time average value from the (demodulated) response frequency time trace. The amplitude response via the H-H technique result is compared to that obtained with a standard direct counting peaks method, where the amplitude is taken as the average of the highest $1/10^{th}$ values.

For the sake of comparison, the amplitude response determined with H-H analysis was taken from the amplitude time trace (demodulated amplitude) in two ways: (i) as the average of the highest $1/10^{th}$ peaks; (ii) as the simple time-average of the time-trace.

The agreement, between equivalent amplitude response measures, is rewarding. The whole curve, including the initial, upper and lower branches are recovered. Some discrepancy at the tail of the lower branch, at $V_r \cong 10$ is observed. However, as will be shown, this relates to a 'chaotic' response behavior.

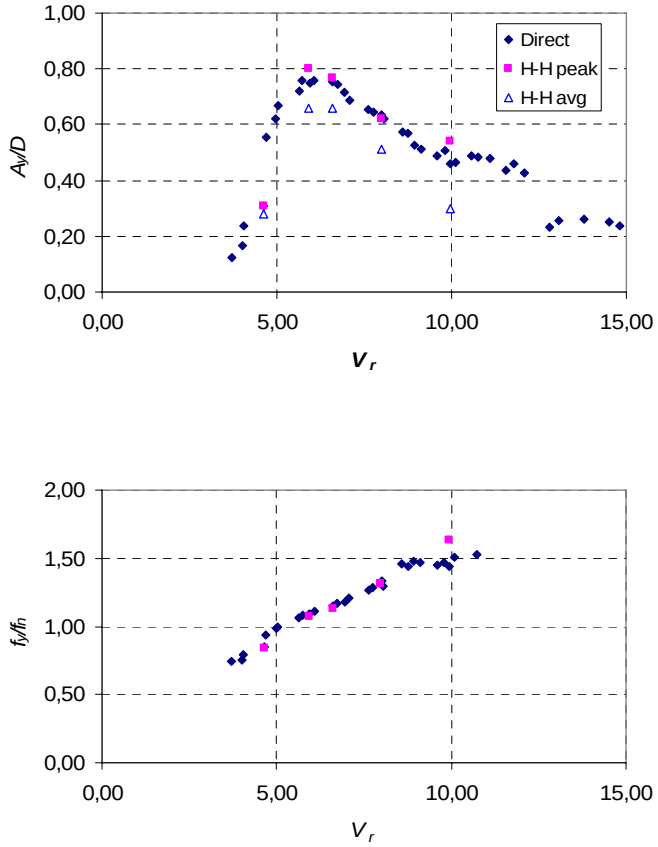

Figure 7. Nondimensional amplitude and frequency. Spring-leaves span fixed. Counting peaks: direct and Hilbert-Huang techniques. ($L_s = 485\text{mm}$; $f_n = 1.19\text{Hz}$ from zero towing speed decaying tests).

In fact, Figure 8 shows an example of a run at $V_r = 6.60$. The amplitude signal is relatively well behaved at the upper branch, as shows the demodulated amplitude, whereas the frequency trace presents small variations with time.

On the other hand, Fig. 9 shows an example of a run at $V_r = 9.95$. The amplitude signal is rather 'chaotic', at the lower branch tail, as testifies not only the demodulated amplitude time trace but, particularly, the strong variation that is observed in the response frequency time trace.

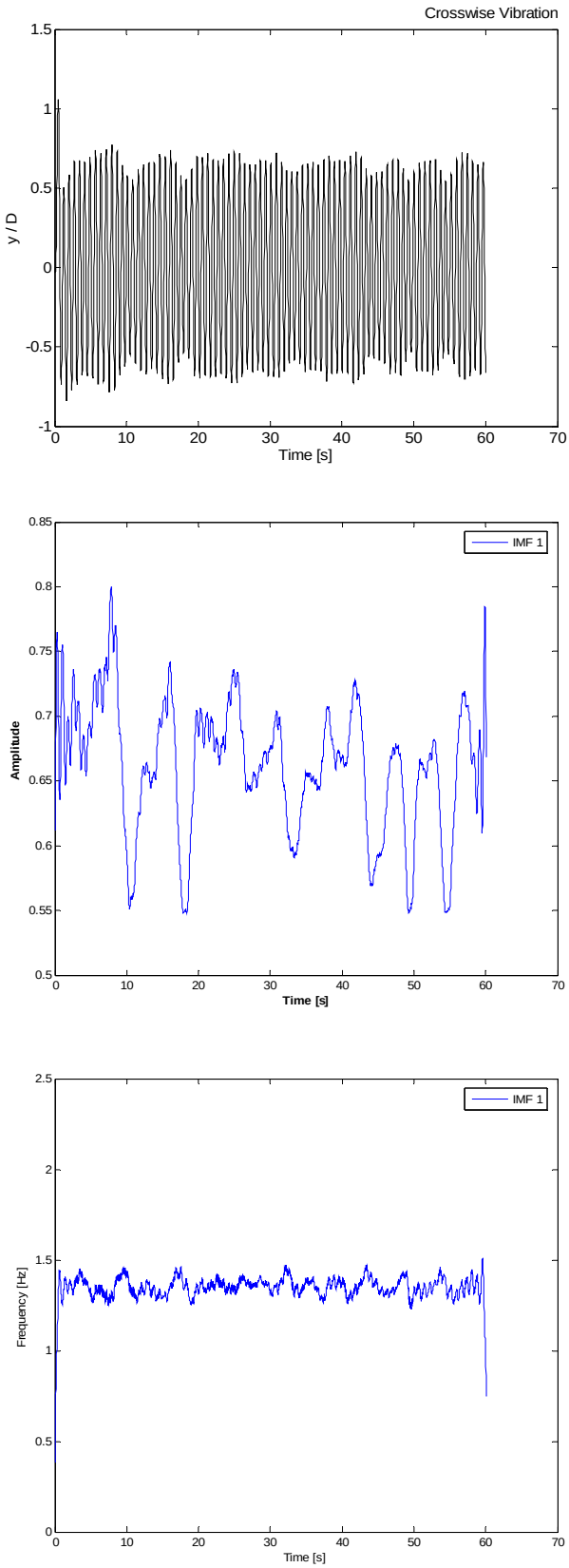

Figure 8. Spring-leaves span fixed. Hilbert-Huang technique. Signal, amplitude and frequency traces. $V_r = 6.60$ **;** $L = 485\text{mm}$; $f_n = 1.19\text{Hz}$ **.**

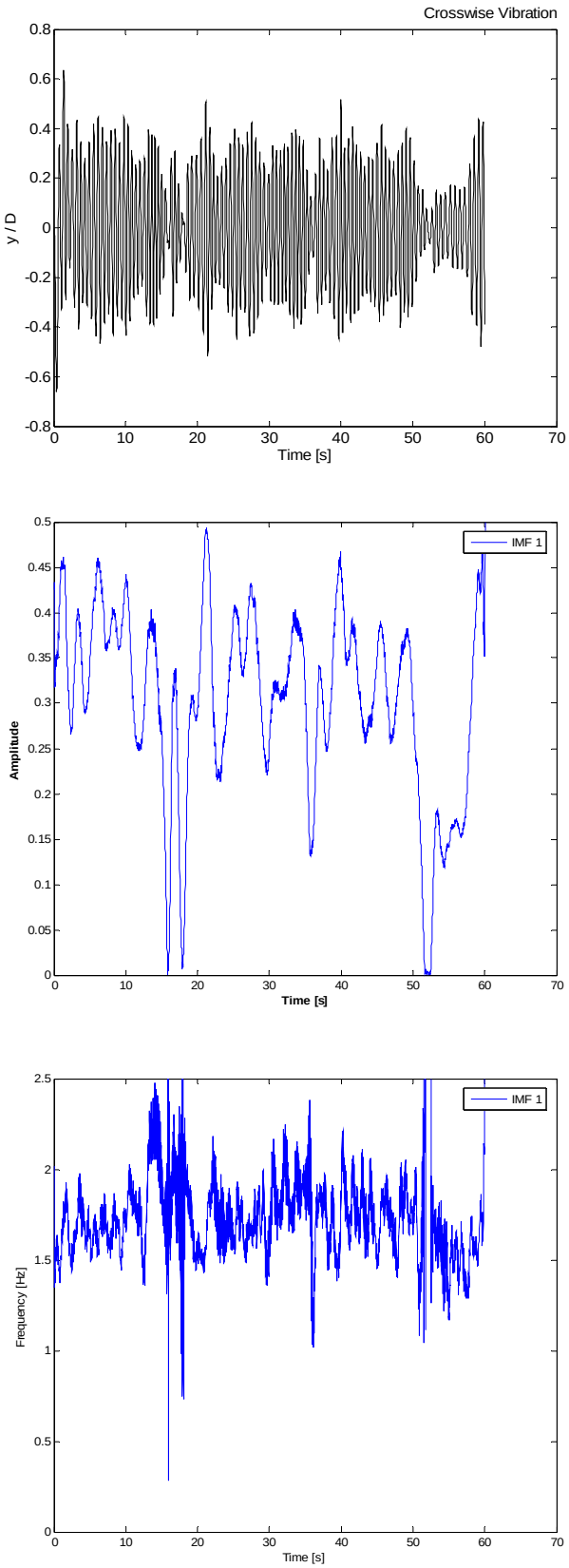

Figure 9. Spring-leaves span fixed. Hilbert-Huang technique. Signal, amplitude and frequency traces. $V_r = 9.95$ **;** $L = 485\text{mm}$; $f_n = 1.19\text{Hz}$ **.**

Runs varying spring-leaves span (i.e., under frequency modulation) and at constant Reynolds numbers

We now turn our attention to a novel experiment procedure. Such a procedure allows to recover the whole VIV response (amplitude and frequency curves) as functions of reduced velocity from a single run an at a fixed Reynolds number.

As anticipated, this is made possible: (i) by modulating the natural frequency in time, so making the reduced velocity to vary during that particular constant velocity run; (ii) by applying the Hilbert-Huang analysis technique to the highly non-stationary signal emerging from that run. Two run conditions were chosen as examples, named N and K, as shown in Table 4, below. Keeping the carriage speed U constant, the instantaneous (slowly-varying) reduced velocity is,

$$V_r(t) = \frac{U}{f_n(t)D} \qquad , \tag{7}$$

The towing tank carriage speed is 0.14m/s in run N and 0.26m/s in run K. These speeds correspond to Reynolds number values 3556 and 6604, respectively. In run N, spring-leaves span varied between 264 and 790mm. In run K, the span length range was 264 to 485mm. In both cases, the clamp speed, imposed with a screw driven by a controlled step-motor, was kept constant at a very small value of 1.0mm/s[3]. With this clamp velocity, reduced velocity varied from 1.83 to 9.03 in run N and from 3.40 to 8.60 in run K.

With the towing tank carriage at rest, the clamp is firstly positioned at the upper position (highest spring-leaves span). The carriage is then smoothly accelerated from rest up to the pre-set speed. After the cylinder response becomes 'stationary', the step motor system is activated, driven the clamp downwards, slowly (and linearly) decreasing the span, hence increasing (nonlinearly) the spring-leaves stiffness and the first natural frequency. When the clamp reaches the lower position, the step motor - and so the clamp motion - is reversed. This procedure allows varying the reduced velocity down and up, continuously, without changing the carriage speed, therefore at a constant Reynolds number.

Table 4. Runs at constant Reynolds number under natural frequency modulation.

Runs	U (m/s)	Re	Span range (mm)	Clamp speed (mm/s)	V_r range
N	0.14	3556	264-790	1.0	1.83-9.03
K	0.26	6604	264-485	1.0	3.40-8.60
M	0.14	3556	264-790	4.0	1.83-9.03

The Hilbert-Huang technique analysis is then applied to the resulting (twice integrated) crosswise displacement signal and the whole VIV response is continuously obtained at each instantaneous reduced velocity value.

[3] Note that the clamp speed is three orders of magnitude lower than the typical bending wave celerity ($c \approx 2L_S f_1$) of the springs, which, in this case, approximately ranges from 960 to 1600mm/s (this may be promptly determined from Fig. 3).

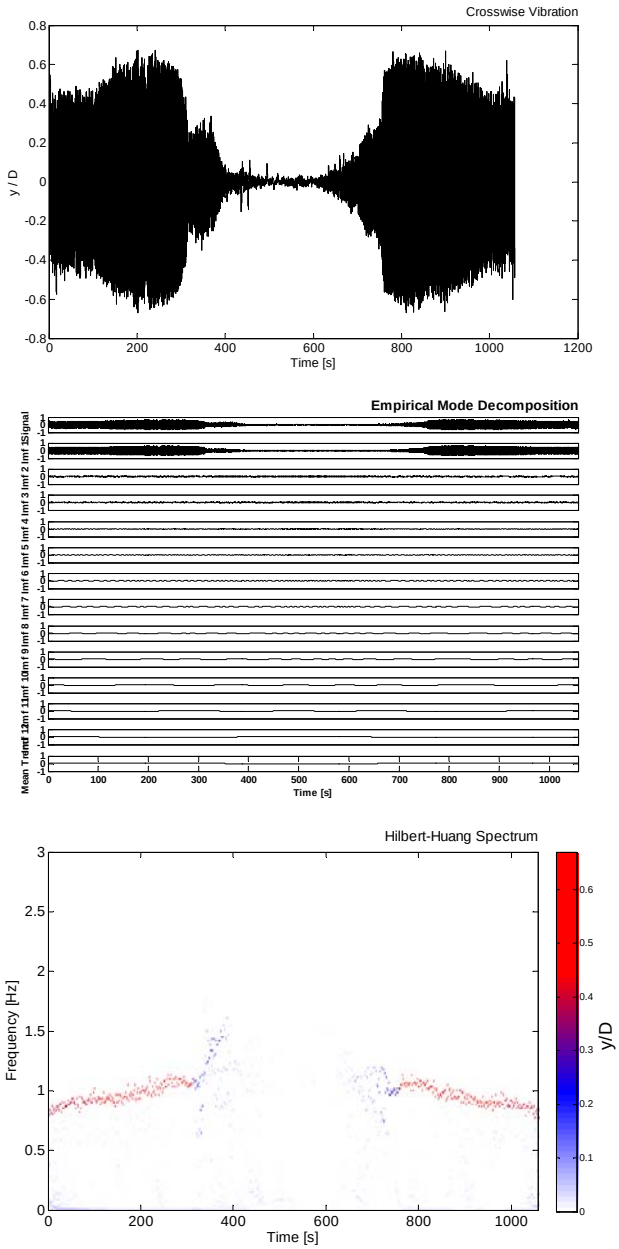

Figure 10. H-H analysis. Crosswise oscillation signal, IMFs and H-H spectrum. Run N3. Modulating natural frequency. Re=3556. Clamp speed 1mm/s.

Figure 10, 11, 12 shows a complete analysis set, for run N3. Figure 10 shows the crosswise vibration, the IMFs and the HH spectrum. The displacement signal is strongly non-stationary, as should be expected. IMF 1 is the most energetic, as observed below, retaining the most important features of the signal. Figure 11 shows the slowly modulated natural frequency imposed by the clamp dislocation, back and forward at 1mm/s. Figure 12 presents the VIV amplitude and frequency time-traces. The demodulated amplitude time trace is relatively well behaved, showing well defined variations during the run, starting from the tail of the lower branch, passing through the

upper branch, the initial branch, 'dying' at low reduced velocities and backwards.

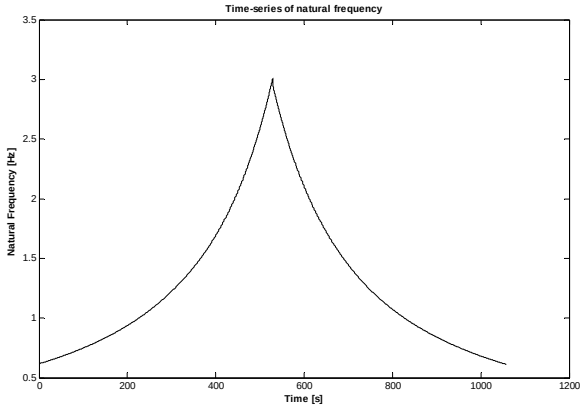

Figure 11. Run N3. Modulating natural frequency. Clamp speed 1mm/s.

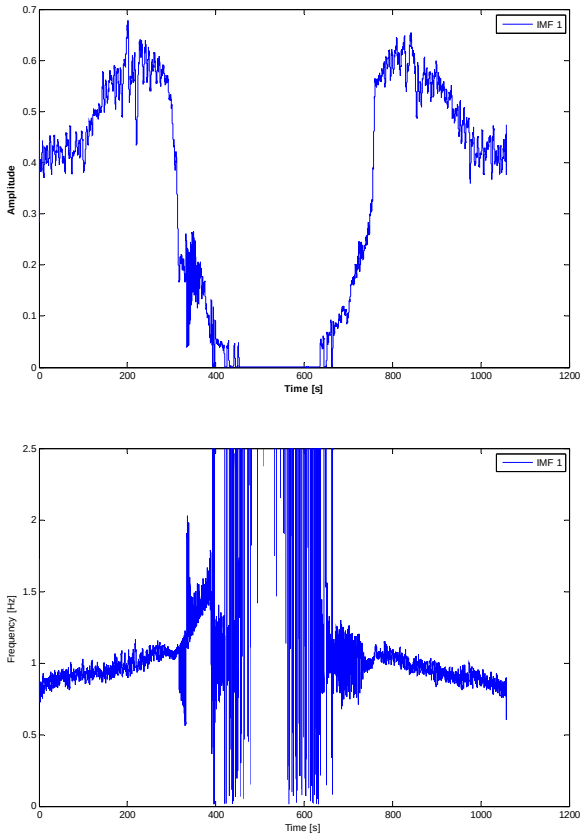

Figure 12. H-H analysis. Amplitude and frequency traces. Run N3. Modulating natural frequency. Re=3556.

On the other hand, the frequency time trace presents very high (quantitatively meaningless but qualitatively meaningful) values, when the amplitude is very small, at low reduced velocities. This fact is clear in the frequency response curve, shown in Fig. 13. This figure shows a novel result: the whole - continuously obtained - VIV response, at a constant Reynolds number. The black line is the response with decreasing reduced velocity, whereas the red line corresponds to the increasing regime. Remarkable is the hysteresis clearly observed when passing from the upper to the initial branch or vice-versa. Such hysteretic behavior may be also noticed observing the asymmetric modulation of the displacement signal in Fig. 10 or from the asymmetric demodulated amplitude time trace in Fig. 12.

Figure 14 exemplifies the repeatability of the method. A twin run, named N5, shows almost the same response result as N3. In this case, the hysteresis is even more visible. Such hysteresis will be shown to be more pronounceable for larger rates of natural frequency modulation.

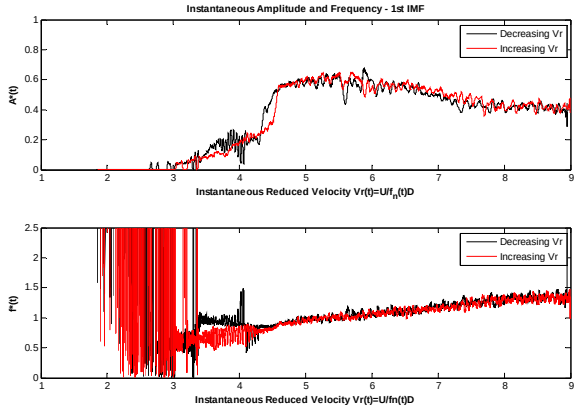

Figure 13. H-H analysis. Amplitude and frequency vs. decreasing and increasing $V_r(L(t))$. Run N3. Modulating natural frequency. Re=3556. Clamp speed 1mm/s.

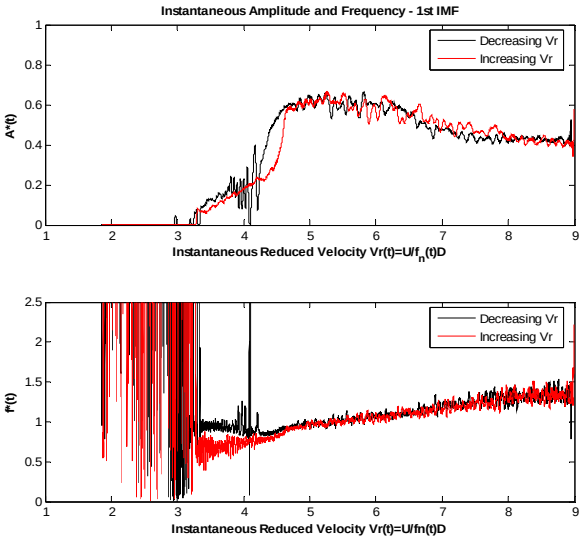

Figure 14. H-H analysis. Amplitude and frequency vs. decreasing and increasing $V_r(L(t))$. Run N5. Modulating natural frequency. Re=3556. Clamp speed 1mm/s.

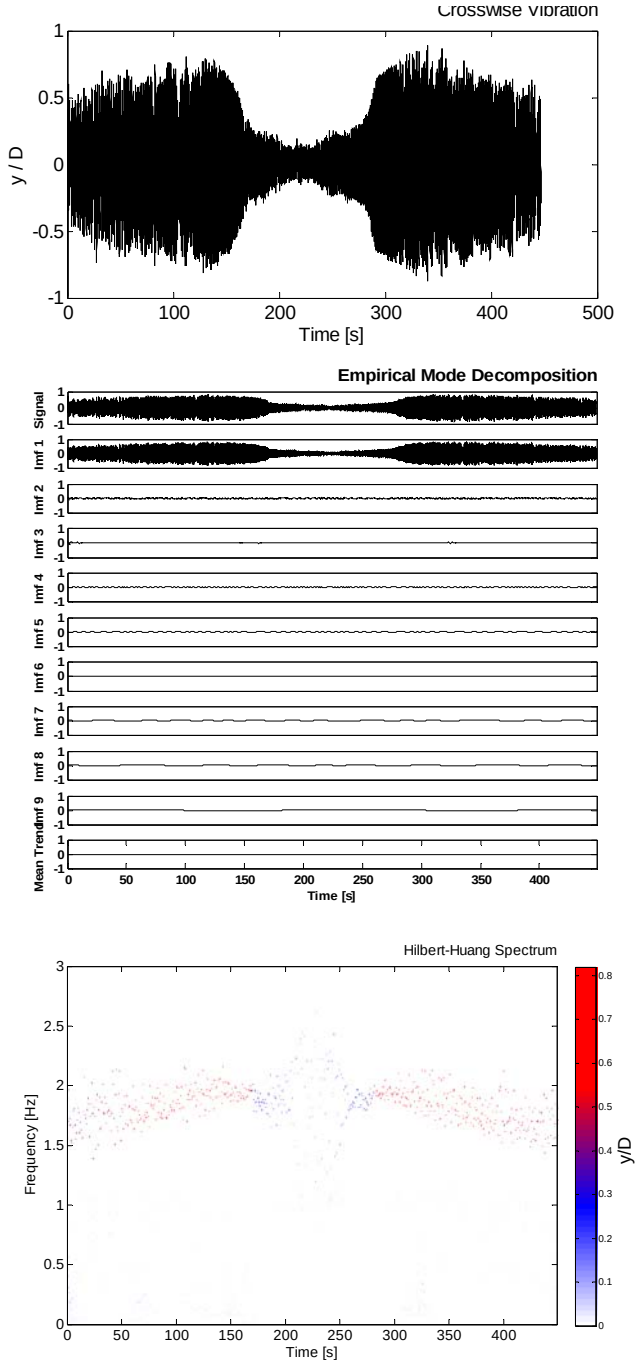

Figure 15. H-H analysis. Crosswise oscillation signal, IMFs and H-H spectrum. Run K6. Modulating natural frequency. Re=6604. Clamp speed 1mm/s.

Figures 15 and 16 exemplify a K run, at a higher Reynolds number, $\mathrm{Re} = 6604$, but at the same natural frequency modulation rate. Similar results are obtained. However, upper and lower branches are not so well distinguishable and both, amplitude and frequency responses are more pronounceably ragged. This is particularly true at high reduced velocities. Nevertheless, the general trend is captured quite well. Particularly, the increasing of the peak response value with Reynolds number is evident (by comparing with Fig. 13 or 14), as should be expected, in accordance to the comprehensive study by Govardhan and Williamson [3].

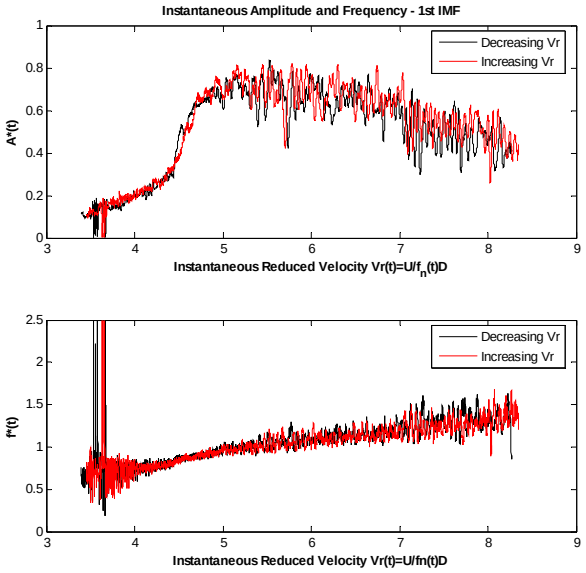

Figure 16. H-H analysis. Amplitude and frequency vs. decreasing and increasing $V_r\,(L(t))$. Run K6. Modulating natural frequency. Re=6604. Clamp speed 1mm/s.

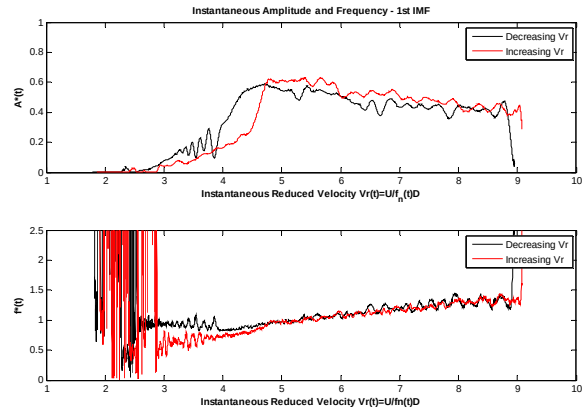

Figure 17. H-H analysis. Amplitude and frequency vs. decreasing and increasing $V_r\,(L(t))$. Run M5. Modulating natural frequency. Re=3556. Clamp speed 4mm/s.

A point deserves further discussion: the peak values attained in the modulated frequency experiments are relatively lower if compared to what should be expected from classical experiments. In the present case the mass-damping parameter, defined in Govardhan and Williamson [3], takes values lower than $\alpha = (m^* + C_a)\zeta \approx 0.025$. Govardhan and Williamson's Fig. 18 would then lead to an amplitude peak $A^* \cong 0.85$ at $\mathrm{Re} = 3556$ and to $A^* \cong 0.95$ at $\mathrm{Re} = 6604$. Instead, the lower values, $A^* \cong 0.65$ and $A^* \cong 0.75$, are readable from Figures 12 (or 13) and 15. On the other hand, our present regular (constant span length, variable Reynolds number) experiment yielded a peak value $A^* \cong 0.8$, at $V_r \cong 6$, i.e., at $\mathrm{Re} \cong 4600$, as

can be seen from our Fig. 7, in contrast to the expected value, $A^* \cong 0.9$. The reason for such a difference is not yet clear.

However, the small decreasing trend in amplitude peak, in the slowly natural frequency modulation technique, seems to be related to the modulation rate of the natural frequency. In fact, Figure 17 shows a VIV response curve, at the same constant Reynolds number, but at a higher natural frequency modulation rate. The clamp speed is now 4mm/s. Additionaly, more remarkable than the slight decreasing trend in amplitude peak, the higher natural frequency modulation rate smoothes the amplitude response curve and turns the hysteresis loop even more pronounced. These particular qualitatively features are phenomenological, not related to the HH analysis technique. They also appear in VIV simulations using models that couple Van der Pol and Mathieu oscillators and is related to the to the wake memory. A future paper will address such a point and its implications concerning practical applications.

CONCLUDING REMARKS

This work presented a new apparatus and a novel experimental technique on VIV. The device enables to carry VIV experiments under frequency modulation and is designed to rigid or flexible cylinders assemblies. The application of the Hilbert-Huang spectral analysis technique was shown suitable to treat the emerged nonlinear and non-stationary responses. Applications of such technique on transient VIV phenomena, such as those provoked by modal competition and modal switching, observable in riser dynamics are devised.

Through slow natural frequency modulation, a novel and interesting result was obtained: whole VIV responses (amplitude and frequency curves vs. reduced velocity) at constant Reynolds number runs. More over, experimental evidences of amplitude and hysteresis dependence on the frequency modulation rate were also observed. Much more remains to be investigated though and many technical points will be addressed in further works.

ACKNOWLEDGMENTS

The authors acknowledge CNPq, the National Research Council, and ANP (the Petroleum National Agency). Our thanks to IPT, Technological Research Institute of São Paulo State, especially, to Dr. Carlos Padovezi, IPT Head of the Naval & Ocean Engineering Center, who kindly offered the Towing Tanking facilities. The authors also thank the technicians Mr. Mario L. da Silva and Leoclides David, as weel as Mrs. Rosianita Balena, PhD student, for their help with the experiments. Finally, the authors thank the reviewers for their very constructive suggestions and enlightening comments.

REFERENCES

[1] Chaplin, J.R., Bearman P.W., Huarte, F.J.H., Pattenden, R.J., 2005, “Laboratory Measurements of Vortex-Induced Vibrations of a Vertical Tension Riser in a Stepped Current”, *J of Fluids and Structures*, Vol. 21, pp. 3-24.

[2] Swithenbank, S.B., Marcollo, H., Vandiver, J.K., 2007, “Time-sharing of Frequencies in High-Mode Number Vortex Induced Vibrations, BBVIV5, *5th Conference on Bluff Body Wakes an Vortex-Induced Vibrations*, 12-15 Dec, Costa do Sauípe, Brazil, pp. 51-55.

[3] Govardhan, R.N., Williamson, C.H.K., 2006, “Defining the ‘Modified Griffin Plot’ in Vortex-Induced Vibration: Revealing the Effect of Reynolds Number Using Controlled Damping”, *J of Fluid Mechanics*, Vol. 561, pp.147-180.

[4] Vandiver, J.K., 2007, “Insights on the Flow-Induced Vibration of Flexible Cylinders”, *5th Conference on Bluff Body Wakes an Vortex-Induced Vibrations*, 12-15 Dec 2007, Costa do Sauípe, Brazil, pp. 39-42.

[5] Silveira, L.M.Y, Martins, C.A., Cunha, L.D, Pesce, C.P., 2007, “An Investigation on the Effect of Tension Variation on VIV of Risers”, Proceedings of OMAE’07, *26th Int. Conference on Offshore Mechanics and Arctic Engineering*, June 10-15, San Diego, USA.

[6] Lucor, D, Triantafyllou, M.S., 2008, “Riser Response Analysis by Modal Phase Reconstruction”, *J of Offshore Mechanics and Arctic Engineering*, Vol. 130, p. 581-586

[7] Kaasen KE, 2002, “On Identification of VIV Modes from Measurements”, 12th *Int. Offshore and Polar Engineering Conference*, Vol. 3, pp. 827-833.

[8] Hover, F.S., Miller, S.N., Triantafyllou, M.S., 1997, “Vortex-Induced Vibration of Marine Cables: experiments using force feedback”, *J of Fluids and Structures*, Vol. 11, pp. 307-326.

[9] Kobayashi, S., Nakabayashi, M, Kobayashi, R., Morikawa, H., 2007, “Flow around Propulsion Mechanism using Fin with Dynamic Variable-Effective-Length Spring”, *17th Int. Offshore and Polar Engineering Conference*, Lisbon, Portugal, pp. 1150-1154.

[10] Fujarra, A.L.C., Pesce, C.P., 2002, “Added Mass of an Elastically Mounted Rigid Cylinder in Water Subjected To Vortex-Induced Vibrations”, *21stInt. Conference on Offshore Mechanics and Arctic Engineering*, Oslo, Norway, 23-28 June.

[11] Pesce, C.P. and Fujarra, A.L.C., 2000, “Vortex-Induced Vibrations and Jumping Phenomenon: An experimental investigation with a clamped flexible cylinder in water”, *Int. J of Offshore and Polar Engineering*, Vol.10 (1), pp. 26-33.

[12] Fujarra, A.L.C., Pesce, C.P., Flemming, F. and Williamson, C.H.K., 2001"Vortex-Induced Vibrations of a Flexible Cantilever", *J of Fluids and Structures*. Vol. 15, no. 3/4, pp. 651-658.

[13] Pesce, C.P., Fujarra, A.L.C, Kubota, L., 2006, “The Hilbert-Huang Spectral Analysis Method Applied to VIV”, Proceedings of OMAE’06, *25th Int. Conference on Offshore Mechanics and Arctic Engineering*, June 4–9, Hamburg, Germany.

[14] Huang, N.E. et al, 1998, “The Empirical Mode Decomposition and the Hilbert Spectrum for Non-linear and Non-stationary Time Series Analysis”, *Proc. R. Soc. Lond. A*, **454**, pp. 903-995.